

Photopolymerization Kinetics and Dynamic Mechanical Properties of Silanes Hydrolyzed without Evolution of Byproducts. Tetrakis[(methacryloyloxy)ethoxy]silane—Diethylene Glycol Dimethacrylate

Mustafa Uygun,^{†,‡} Wayne D. Cook,^{*,†} Cornelis Moorhoff,[†] Fei Chen,[†] Claudia Vallo,[§] Yusuf Yagci,[‡] and Marco Sangermano^{||}

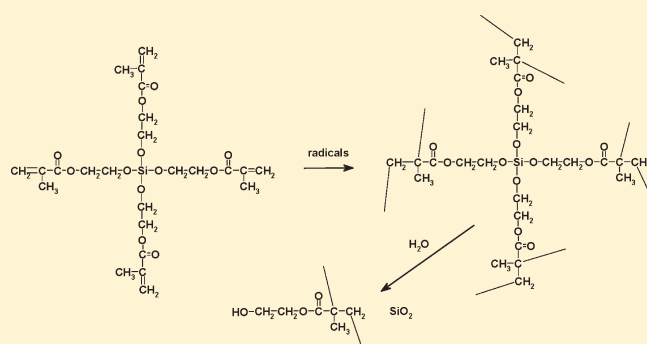
[†]Department of Materials Engineering, Monash University, Clayton, Victoria 3800, Australia

[‡]Department of Chemistry, Istanbul Technical University, Maslak 34469, Istanbul, Turkey

[§]INTEMA, Universidad Nacional de Mar del Plata, Mar del Plata 7600, Argentina

^{||}Department of Materials Science and Chemical Engineering, Politecnico di Torino, Torino 24-10129, Italy

ABSTRACT: The temperature dependence of photopolymerization kinetics of tetrakis[(methacryloyloxy)ethoxy]silane (TetMESi) was compared with an analogue, diethylene glycol dimethacrylate and their copolymers. In all cases, the kinetics are controlled by the temperature dependence of the propagation step, the effect of diffusion on radical termination, the effect of rising glass transition during cure, and topological restraint on complete conversion. The glass transition regions of these polymers were very broad, suggesting their use in high temperature applications. NMR of the TetMESi monomer, and FTIR and water sorption measurements during exposure to water of the TetMESi-based polymers showed that the Si—O—C bond was slowly hydrolyzed, resulting in water-swollen polymers containing poly(hydroxyethyl methacrylate) which reduced the glass transition temperature and narrowed the glass transition region. UV—vis spectroscopic studies showed that during exposure to water, SiO₂ nanoparticles or nanostructures were formed from the condensation of the silanol groups formed during the hydrolysis of TetMESi.



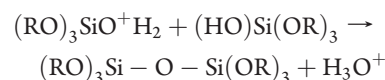
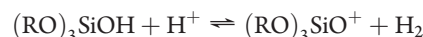
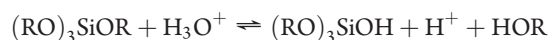
INTRODUCTION

Over the last three decades, hybrid inorganic—organic materials have attracted increasing attention in the field of material science due to their extraordinary properties, which arise from the synergism between the properties of the components. Hybrid materials are classified as type-I and type-II hybrids according to the interaction between inorganic and organic moieties.¹ Type-I hybrids contain weak bonds such as van der Waals, ionic, or hydrogen bonds, whereas type-II hybrids contain strong covalent bonds. Hybrid materials have generally been produced by sol—gel processing through homogeneous hydrolysis and condensation reactions of metal alkoxides.

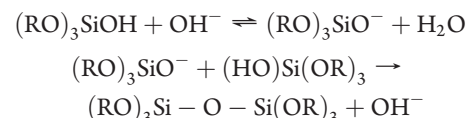
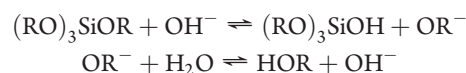
Silane based UV-curable monomers are widely used as pressure sensitive adhesives and weather resistant coatings due to their low surface energy, low polarity, chemical inertness, and long-term weather resistance.^{2–4} However, the photopolymerization kinetics of their formulations and the properties of the cured products have scarcely been investigated.

In the sol—gel process, the gelation of metal-alkoxides, including silanes, involves two steps: hydrolysis of the metal—alkoxide

and condensation of the silanol groups^{5–8} by either acid



or base



Received: December 20, 2010

Revised: February 20, 2011

In fairly strong acid catalyzed conditions, the condensation (polymerization) process is faster than the hydrolysis reaction and so linear chains are initially formed, which then form an open gel structure, whereas when fairly strong basic conditions are used, the hydrolysis is faster than the condensation reaction and so particles are formed.⁶ At low levels or in the absence of a catalyst, this situation is less clear,⁹ but Brinker and Scherer⁷ conclude that these conditions produce intermediate structures as originally suggested by Schaefer and Keefer.¹⁰

The conventional sol–gel process has several disadvantages including a large volume shrinkage resulting from the removal of solvents and small molecular byproducts of the hydrolysis and polycondensation reactions such as water and alcohol. Recently a number of researchers have addressed this problem^{11–23} by replacing the solvent-based alkoxides, such as methoxy and ethoxy, with polymerizable alkoxide groups. Because this process involves the polymerization of the hydroxyl monomer, the volume shrinkage can be considerably reduced or eliminated.

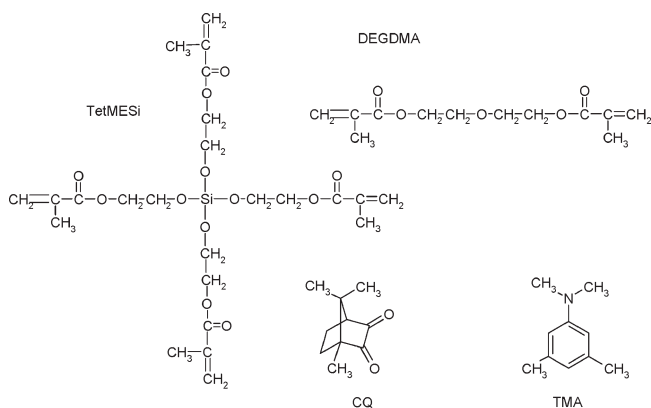
There have been numerous studies of silanes containing a single reactive functional group[†] such as 3-(trimethoxysilyl)propyl methacrylate²¹ or (3-glycidoxypropyl)trimethoxysilane^{24,25} but far fewer investigations with silanes having three of four reactive groups. Davidson et al.¹⁵ synthesized di- and tri(meth)acrylate silanes and showed that they had high photopolymerization rates and suggested their use as surface coatings. Novak and Davies¹¹ studied a tetraacrylate silane suitable for the formation of highly uniform monolithic glasses and inorganic ceramic composite and monitored the development of mechanical properties during their simultaneous photopolymerization and hydrolysis by water (20–40% in stoichiometric excess) in the presence of NaF catalyst. According to these workers¹¹ it was considered important that the photopolymerization and hydrolysis/condensation rates were comparable because systems with faster hydrolysis/condensation rates were claimed to produce opaque, brittle glasses that shrink due to the evaporation of unreacted monomer, whereas it was claimed that phase separation of the monomer and water occurred with fast photopolymerization rates causing loss of clarity. Kloosterboer and Touwslager²⁰ patented the use of a tetraacrylate silane for use in a liquid display device and observed that the dynamic mechanical properties of the polymerized material exhibited a broad glass transition region and that after hydrolysis and drying the material was transparent. Some other interesting multifunctional silane systems are those of Spange and Grund²³ involving the cationic polymerization and cationic hydrolysis/condensation of tetrafururyloxysilane and of spirobis-benzodioxasilane and by Novak^{12,13} on the ring-opening metathesis polymerization of cyclic alkenylsilane monomers.

In this study, we report the polymerization kinetics and dynamic mechanical properties of a silane based hybrid material, namely tetrakis[(methacryloyloxy)ethoxy]silane, by itself and in copolymerization with diethylene glycol dimethacrylate, and we investigate their spectroscopy, water uptake, and viscoelastic behavior in an aqueous environment.

EXPERIMENTAL SECTION

The tetrafunctional silane monomer studied was tetrakis[(methacryloyloxy)ethoxy]silane (TetMESi or 2-propenoic acid, 2-methyl-, silanetetrayltetrakis(oxy-2,1-ethanediyl) ester) and was prepared by our group in a manner similar to that described in the literature.¹⁵ Silicon tetrachloride was reacted with hydroxyethyl methacrylate (HEMA) at room temperature in anhydrous dichloromethane using a slight stoichiometric excess of pyridine to absorb the HCl generated.

Scheme 1. Structures of Materials Used



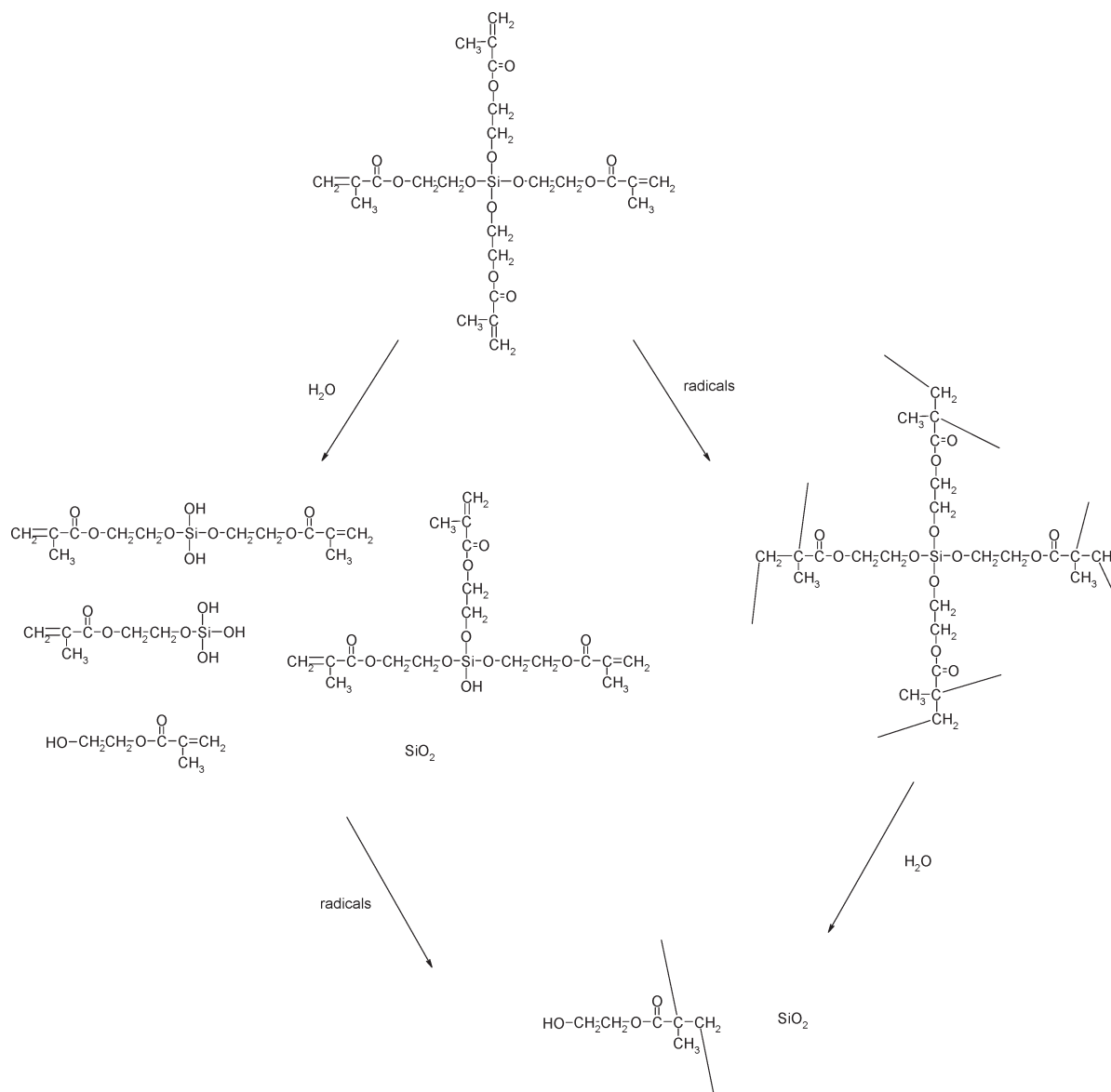
After 16 h, the dichloromethane was removed by rotary evaporation, and the pyridinium hydrochloride salt was filtered off. ¹H NMR analysis with a 300 MHz Bruker instrument in CDCl₃ gave the following peaks: δ = 1.895 (dd, *J* = 1.2, 1.5 Hz, 4 × 3H), 3.966 (m, 4 × 2H), 4.199 (m, 4 × 2H), 5.523 (sm, 4 × 1H), 6.085 (sm, 4 × 1H) ppm. ¹³C NMR (75 MHz, CDCl₃): δ = 18.26 (Me), 61.92 (O—CH₂), 65.18 (O—CH₂), 125.72 (H₂C=), 136.22 (C=), 167.23 (C=O) ppm. The NMR analysis also revealed that the TetMESi contained 0.07 wt % residual pyridine and this has relevance to the catalysis of the hydrolysis of TetMESi by water.

The structure of the tetramethacrylate, TetMESi, is analogous to the dimethacrylate, diethylene glycol dimethacrylate (DEGDMA, supplied by Sartomer USA), in that the mass per methacrylate unit is similar (121 g/mol of methacrylate units in DEGDMMA versus 136 g/mol for TetMESi), and so DEGDMMA was chosen for comparison with the silane monomer. TetMESi and DEGDMMA were homo- and copolymerized using 0.5 wt % (±)-camphorquinone (CQ, supplied by Sigma Aldrich Pty Ltd.) as a visible light photoinitiator and 0.30 wt % *N,N,N',N',3,5*-tetramethylaniline (TMA, supplied by Sigma Aldrich Pty Ltd.) as photoreducer. The TMA photoreducer and the residual pyridine in the TetMESi synthesis are basic with *pK_b* (aqueous, 20–25 °C) values of 8.9 for *N,N*-dimethylaniline (which is analogous to TMA) and 8.8 for pyridine,²⁶ so that the pH of an aqueous solution of these species should be approximately 9 and so only slightly basic. All chemical structures of the materials used are presented in Scheme 1.

Since NMR studies of the hydrolysis of polymerized TetMESi by water are difficult, we studied the hydrolysis of the monomer in a 70/30 w/w blend of TetMESi and acetone-*d*₆ (supplied by Cambridge Isotope Laboratories Inc.). The acetone was used as a NMR spin lock and also as a solubilizer for TetMESi and water. To this blend was added 4.63 pph water (6.2 wt % water based on the monomer and equal to the stoichiometric amount required for complete hydrolysis). In addition, since the photoinitiation system contained 0.3 wt % TMA as discussed above, which is basic and was expected to catalyze the hydrolysis, this level was added to the TetMESi/acetone blend. A 300 MHz Bruker ¹H NMR was used to monitor the disappearance of the methylene group of TetMESi (—CH₂—O—Si—) at δ = 3.9 ppm and the emergence of the methylene group of HEMA (—CH₂OH) at δ = 3.7 ppm. The formation of the silica particles was also monitored by visual observation of the development of turbidity of a water-saturated solution of TetMESi (~1.5 wt %). Schematic 2 shows the pathways for polymerization/hydrolysis of TetMESi.

The isothermal photopolymerization studies were conducted under a N₂ atmosphere at various temperatures from –10 to +90 °C using a differential scanning calorimeter (Perkin-Elmer DSC-7 and Intracooler). The instrument was modified to allow the simultaneous irradiation of the sample pans, as previously discussed by Cook.²⁷ The calorimeter was calibrated for temperature and enthalpy using zinc and indium standards. The DSC sample was irradiated with a broad band dental curing light

Scheme 2. Polymerization Pathways of the TetMESi Monomer and Hydrolytic Pathways of the Monomer and Polymer



158 (Visilux, 3M) which produces visible light with the wavelength ranging
 159 from 400 to 500 nm and has a maximum emittance at 470 nm correspond-
 160 ing to the absorption maximum of CQ₂. Due to the fast polymerization rate
 161 of the monomers with this photocuring source, its intensity was reduced by
 162 a factor of 10 by placing a neutral density filter (Schott) between the source
 163 and the fiber optic bundle. The irradiation intensity at the surface of the
 164 DSC pan was measured using an International Light IL1700 radiometer
 165 equipped with a SED033/UVA/W detector and found to be 10.7 mW/
 166 cm². The theoretical heat of polymerization for the methacrylate group
 167 (54.4 kJ/mol)²⁸ was used to calculate the conversion of double bonds from
 168 the experimental heat of polymerization of the monomers.

169 For the preparation of the cured polymer specimens, the monomer
 170 blends and initiators were injected between two glass slides separated by
 171 a 1.4 mm thick silicone gasket and were photocured at 60 °C by the
 172 Visilux source without a filter at an irradiance of 5.1 mW/cm² for 10 min.
 173 The samples were then postcured at 120 °C for 2 h.

174 Cured samples of the TetMESi and DEGDMA and their blends
 175 were exposed to a water vapor saturated atmosphere at 40 °C and
 176 their wt % water uptake (the mass of absorbed water divided by the

177 initial specimen mass) was monitored as a function of time. During the
 178 water uptake experiment, the 1.4 mm thick specimens containing TetMESi
 179 became cloudy as a result of the hydrolysis of the Si-O-C links and the
 180 formation of SiO₂ particles. The progress of the particle formation and thus
 181 light scattering was monitored by measurements of the forward scattered
 182 ultraviolet–visible radiation using a Varian Cary 300BIO UV–vis spectro-
 183 photometer fitted with a DRA-CA-30I sphere accessory. These spectra
 184 were measured from 800 to 200 at 600 nm/min and are presented as the
 185 percent transmission and the apparent absorption (the logarithm of the
 186 inverse fractional transmission) versus the wavelength.

187 Digital optical photographs of the polymers were taken of 1.4 mm
 188 thick samples overlaid on white paper with crisply printed text to
 189 highlight the relative transparency of the materials.

190 The dynamic mechanical properties of the specimens with dimen-
 191 sions of 1.4 mm × 5 mm × 40 mm were measured at 1 Hz by a Perkin-
 192 Elmer DMA 8000 instrument tested in dual cantilever geometry and
 193 using a heating rate of 3 °C/min from −90 to +250 °C. Where it could
 194 be clearly defined, the glass transition temperature (*T_g*) was taken as the
 195 temperature at the peak of the tanδ curve.

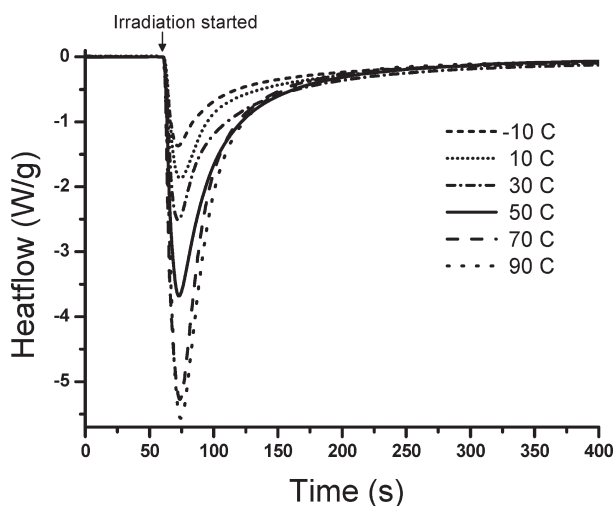


Figure 1. PhotoDSC during the cure of TetMESi with 0.5 wt % CQ and 0.3 wt % TMA at various temperatures.

196 The Fourier transform infrared spectra of monomers and polymers
197 were recorded using a Nicolet 6700 FTIR spectrometer, with a resolu-
198 tion of 4 cm^{-1} , and a Smart Orbit single-bounce diamond attenuated
199 total reflection (ATR) accessory with a diamond crystal.

RESULTS AND DISCUSSION

Photopolymerization. Figure 1 shows the isothermal photo-
polymerization behavior of TetMESi at various temperatures,
and Table 1 lists the maximum heat flow, heat of polymerization,
and methacrylate conversion obtained from this data. As com-
monly found in free radical polymerization, and especially cross-
linking systems,^{27,29–31} the rate is initially very slow but rapidly
rises to a maximum and then decreases, due to the combined
reduction in the initiation efficiency and the rate of termination
by diffusional effects, and the effect of reduction in monomer
concentration. The maximum heat flow rises with increased
temperature, but a change of $100\text{ }^{\circ}\text{C}$ only causes an increase in
rate by a factor of 4. Since the polymerization is photochemically
initiated, this rise in polymerization rate with increased tempera-
ture is probably due to the enhanced rate of propagation.^{27,30,31}

Table 1 also shows that the final conversion also increases with
raised temperature until a plateau value is achieved, but this
maximum value is much less than the full reaction. This type of
behavior is commonly observed when the glass transition tem-
perature of the polymerizing monomer/polymer mixture is close to
the curing temperature^{29–33} and can be explained as follows. At
the start of the polymerization, the T_g of the monomer is low and so the
high molecular mobility in the matrix allows the curing to proceed
without hindrance. As the molecular weight and cross-linking in the
polymer rises, the glass transition temperature rises, but provided
the T_g is below the curing temperature, the molecular mobility still
permits the curing to proceed. When the polymerization causes the
glass transition to approach the curing temperature, the molecular
mobility in the matrix is diminished and so the polymerization rate
slows. With further curing, the increase in T_g restricts molecular
mobility and eventually prevents further polymerization. At
this stage, the T_g attains a plateau value because there is no further
increase in molecular weight or cross-link density. If reactive
groups still remain at this stage, then polymerization can often
be re-established by increasing the curing temperature and thus

Table 1. Cure parameters for the Photopolymerization of TetMESi, DEGDMA, and Their Copolymer at Various Isothermal Curing Temperatures

temperature ($^{\circ}\text{C}$)	peak maximum			
	heat flow (W/g)	time (s)	ΔH (J/g)	conversion (%) [*]
TetMESi				
-10	1.37	72	120	30
10	1.89	74	142	35
30	2.52	73	195	48
50	3.68	73	207	52
70	5.27	73	243	61
90	5.56	74	255	64
50/50 TetMESi/DEGDMA				
-10	1.48	77	137	32
10	2.37	67	171	40
30	3.16	71	237	56
50	4.20	76	235	55
70	5.93	77	245	58
90	6.01	75	236	56
DEGDMA				
-10	0.40	78	110	24
10	0.62	75	186	41
30	0.72	188	168	37
50	1.43	151	207	46
70	1.66	129	170	38
90	2.42	115	204	45

increasing molecular mobility. As a result, the plateau T_g is
closely related to the curing temperature. In the case of a
monofunctional monomer polymerizing into a linear polymer,
the topological ability of a growing chain to react with a
monomer is high and so if the curing temperature exceeds
the maximum attainable T_g , then nearly 100% conversion of
monomer to polymer can be achieved. However, in most
polymer networks, a high level of cross-linking can impose
topological restrictions on the neighboring monomer units or
of propagating chains and prevent the conversion from exceed-
ing a certain limit,^{30,32,34–36} and this is termed the topological
limit. Thus the cure temperature and the attainable glass
temperature are coupled until either the material is fully cured
or topological restrictions prevent further reaction, whereupon
the T_g becomes independent of further increases in curing
temperature, as demonstrated in Table 1 and Figure 1.

Photocuring behavior similar to that shown in Figure 1 was
observed for the 50:50 copolymer of TetMESi and DEGDMA
and for the homopolymerization of DEGDMA, and the curing
parameters are listed in Table 1. Figure 2 compares the iso-
thermal photocuring behavior of TetMESi, DEGDMA, and the
copolymer at $50\text{ }^{\circ}\text{C}$. It is interesting to note that the rate of
polymerization of DEGDMA is much less than that for TetMESi,
which is less than that for 50:50 TetMESi:DEGDMA. This
unusual trend was also observed for these systems at all tem-
peratures between -10 and $+90\text{ }^{\circ}\text{C}$ and may be a result of the
effect of two opposing factors on the rate: radical diffusion and
the relative reactivity of the methacrylate groups. In a free radical
cross-linking system, the rate of translational and segmental

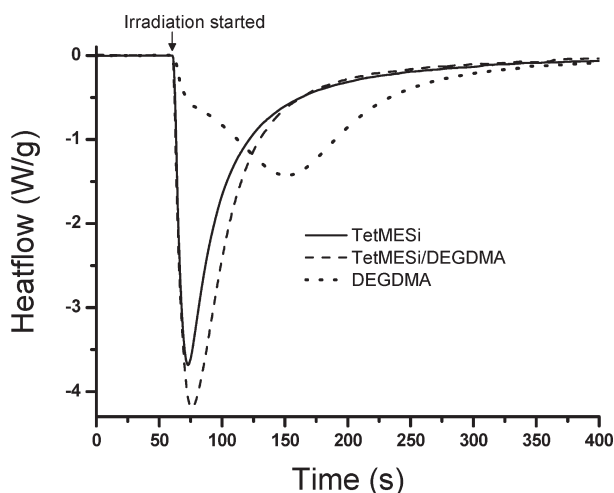


Figure 2. PhotoDSC of TetMESi, 50/50 and DEGDMA and copolymers at 50 °C.

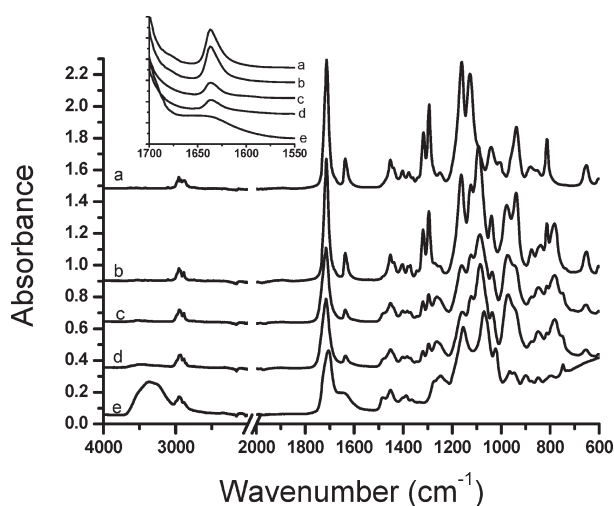


Figure 3. ATR-FTIR of DEGDMA and TetMESi monomers (a and b, respectively) and of TetMESi photocured at 60 °C/10 min (c) or 60 °C/10 min and postcured at 120 °C/2 h (d), and of TetMESi cured at 60 °C/10 min and postcured at 120 °C/2 h followed by exposure to a water saturated atmosphere for 2 weeks (e).

diffusion of the radicals is reduced as the polymerization proceeds^{30,36–38} and so the rate constant for termination decreases dramatically during the reaction and particularly at the stage of gelation. The monomer that has the higher number of functional groups, TetMESi, should gel at a lower conversion than DEGDMA, and this should cause an earlier and more dramatic reduction in the termination rate and thus a higher polymerization rate of the TetMESi/DEGDMA blend compared with DEGDMA. However, the reactivity of the methacrylate groups in TetMESi may be less than those on DEGDMA and this may cause the decrease in rate of TetMESi compared with the TetMESi/DEGDMA blend, as is observed in Table 1.

Table 1 also reveals that the maximum conversion is higher for TetMESi and the 50:50 blend than for DEGDMA. This is somewhat surprising since the DEGDMA is difunctional while TetMESi is tetrafunctional and so it might be expected that topological restrictions in the final stages of reaction would be more important for the latter. One explanation for this behavior is that the

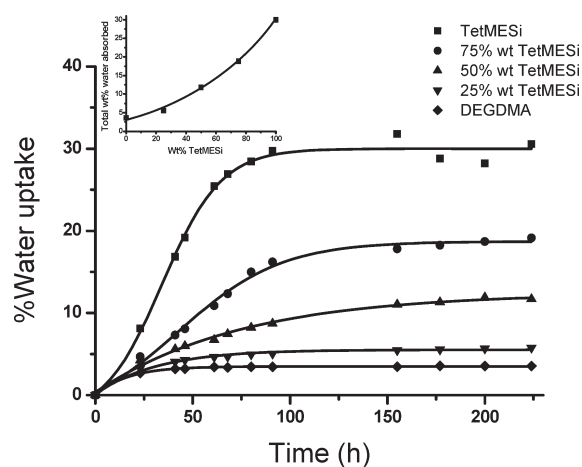


Figure 4. Water vapor uptake of the polymers formed from TetMESi, DEGDMA, and their copolymers at 40 °C. The inset shows the variation of the equilibrium water uptake versus composition.

additional flexibility of the $-\text{O}-\text{Si}-\text{O}-$ bond in the TetMESi allows the methacrylate additional ability for reaction, in the same manner that the presence of the additional ethylene oxide unit in triethylene glycol dimethacrylate provided fewer topological restrictions to polymerization compared with DEGDMA.³⁶

Hydrolysis. Figure 3 shows the FTIR ATR spectra of the TetMESi and DEGDMA monomers. Using the functional group characteristic frequencies³⁹ and by comparison of the spectra of TetMESi with DEGDMA, and also other oligo(ethylene glycol) dimethacrylates, it can be concluded that TetMESi exhibits the characteristic peaks at ~ 2900 (C–H stretch), 1715 (ester carbonyl stretch), 1640 (carbon double bond stretch), 1160 (ester $-\text{C}-\text{O}-\text{CH}_2$ stretch), 1130 ($\text{CH}_2-\text{O}-\text{Si}$ stretch), 1090 (C–O–Si stretch), and 980 cm^{-1} (C–O–Si stretch). As expected, DEGDMA monomer has a similar spectrum but without the peaks at 980 and 1090 cm^{-1} . After photocuring at 60 °C, the vinylidene absorption at 1640 cm^{-1} is greatly reduced and results in $\sim 62\%$ conversion and with postcuring at 120 °C reaches $\sim 68\%$ conversion, which are consistent with the photo-DSC data in Table 1. As discussed above, the pH of an aqueous solution of the amines present in the polymers prepared with TetMESi is expected to be only slightly basic and so the hydrolysis of the monomer is expected to produce silica-based structures intermediate between particles and a silica network. After the polymer has been exposed to saturated water for 2 weeks at 40 °C, new peaks appear at 3350 cm^{-1} due to the water swelling the polymer and at 1065 cm^{-1} due to the Si–O–Si bonds in silica. At the same time, the $\text{CH}_2-\text{O}-\text{Si}$ peak at 1130 cm^{-1} disappears due to its hydrolysis while the stretch of the ether link in the ester at 1160 cm^{-1} remains.

Water vapor absorption experiments were performed with the polymers of TetMESi, DEGDMA and their blends and the kinetics are given in Figure 4. The polymer of TetMESi absorbed a very high amount of water (approximately 30 wt % uptake) and this can be attributed to the water required (6.2 wt % water) for hydrolysis of the polymer to poly(hydroxyethyl methacrylate), hydroxyethyl methacrylate (HEMA) monomer and silica, plus the amount of water that the poly(hydroxyethyl methacrylate) and HEMA monomer absorbs. Hodge et al.⁴⁰ reported that the water uptake of poly-HEMA was approximately 37 wt % water at 25 °C while Dimarco et al.⁴¹ obtained 40 wt % (presumably at room temperature) and Kolarik and Janacek⁴² obtained 46 wt % (presumably at room temperature), which is considerably higher



Figure 5. Photographs of cured 1.4 mm thick specimens (located at the bottom of the images) on top of a white printed card, indicating the level of transparency of (a) polymerized TetMESi, (b) polymerized TetMESi after hydrolysis with water vapor, and (c) polymerized TetMESi after hydrolysis and drying.

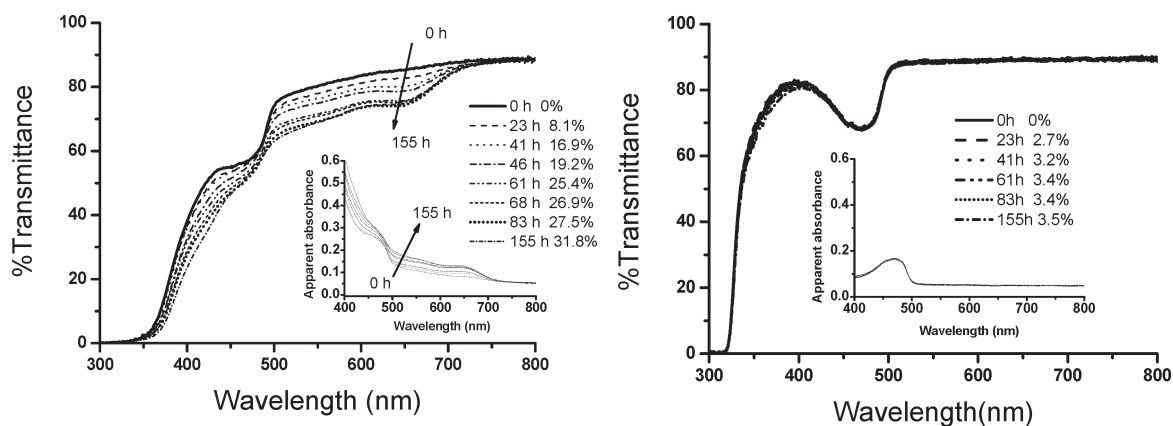


Figure 6. (a) UV-vis data taken with an integrating sphere as the polymerized TetMESi absorbed water and became hazy. (b) UV-vis data taken with an integrating sphere as the polymerized DEGDMa absorbed water but remaining transparent.

than the value determined here. Sideridou and Karabela⁴³ have measured the water uptake of a 31 wt % (50:50 mol %) copolymer of HEMA and triethylene glycol dimethacrylate (which has a structure similar to that of DEGDMa) and obtained a value of 11 wt % at 37 °C, which is also higher than the interpolated value of 8% obtained from Figure 4. The reason for these differences may be due to two effects. As noted by Kolarik and Janacek,⁴² poly-HEMA swollen in liquid water forms two phases (bound water and free water), and it is possible that our samples do not contain free water because they were saturated by water vapor and not by immersion in the liquid. In addition, D'Agostino et al.⁴⁴ also observed a reduction in water absorption with addition of nanosilica particles in poly-HEMA and this effect may apply to our system of poly-HEMA and silica.

Figure 4 also shows that the equilibrium water uptake is a nonlinear function of the weight percentage of TetMESi, which is similar to that found by Hodge et al.⁴⁰ for copolymers of HEMA and 2-ethoxyethyl methacrylate.

As shown in Figure 5, the specimens of polymerized TetMESi, its hydrolyzed form, and the specimen after redrying are relatively transparent as noted by Kloosterboer and Touwslager²⁰ for the acrylate analogue of TetMESi. However, close inspection of the hydrolyzed polymers did show evidence of a slight haze due to the precipitation of SiO₂ nanoparticles or nanostructures. Assuming full hydrolysis of the polymer, 10 wt % of silica would be formed in the poly(HEMA) matrix. Further evidence of the formation of a separate silaceous phase was obtained from UV-vis spectroscopy by collecting the transmitted and forward scattered radiation using an integrating sphere; these data are shown in Figure 6a and are presented as the percent of transmitted and forward scattered radiation and as the apparent absorbance (the logarithm of the inverse fractional transmittance). The spectrum for the unhydrolysed silane polymer showed absorptions due to residual levels of the CQ photoinitiator

(maximum at 470 nm) and absorption below 400 nm due to residual impurities in the original monomer and in the TMA. Upon exposure to the water vapor, the transmittance decreases predominantly near 650 nm and near 420 nm and this is probably due to scattering of the silica nanoparticles or nanostructures.^{45,46} In contrast, the spectra from the DEGDMa polymer (Figure 6b) is virtually unaffected by the absorption of water because no new silica phase is formed. Copolymers of TetMESi with DEGDMa showed spectra midway between that of the two components.

The kinetics of formation of the SiO₂ is controlled by the diffusion rate of the water into the polymer matrix and of the rates of hydrolysis of the Si-O-CH₂ groups and condensation reaction of the silanol groups. As shown by the DSC data (Table 1) and the DMTA data presented below, the TetMESi polymer is glassy at room temperature whereas the swollen poly(HEMA) byproduct is rubbery and so water absorption is expected to be slow and via case II diffusion, otherwise known as relaxation-controlled transport,⁴⁷ where the water profile as a function of distance into the specimen is rather square. An approximate measure of the rate of silica formation can be obtained when the change in apparent absorbance, in the region from 550 and 600 nm, is 50% of the total change and for TetMESi this appears to be approximately 50 h based on the data in Figure 6a). This is similar to the time of 37 h for the water absorption to attain 50% of its final value (approximately 900 min or 15 h; see Figure 4) but is considerably greater than the time for 50% hydrolysis of the monomer (see Figure 7), as would be expected because the time for water diffusion in the latter is minimal.

Dynamic Mechanical Thermal Analysis. The DMTA of the polymers from TetMESi, DEGDMa and the 50/50 copolymer are shown in Figure 8. In all cases, the glass transition region is very broad and the modulus remains high up to 250 °C. The tan δ is also seen to be very low, and the maximum tan δ is only

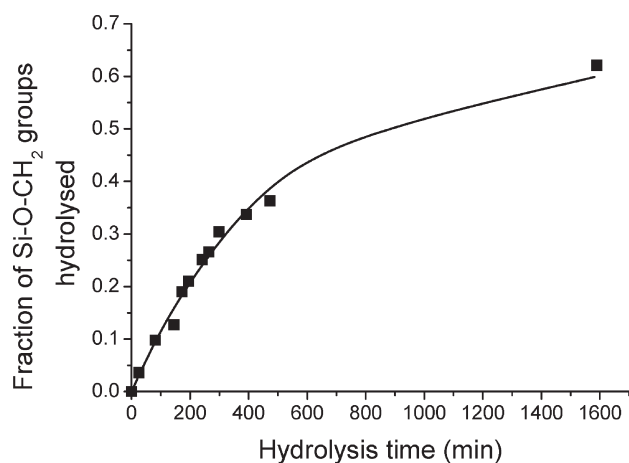


Figure 7. Kinetics of hydrolysis of the TetMESi monomer at 25 °C in a 70/30 mixture of TetMESi/acetone and 0.3 wt % TMA, and containing the stoichiometric amount of water required for hydrolysis.

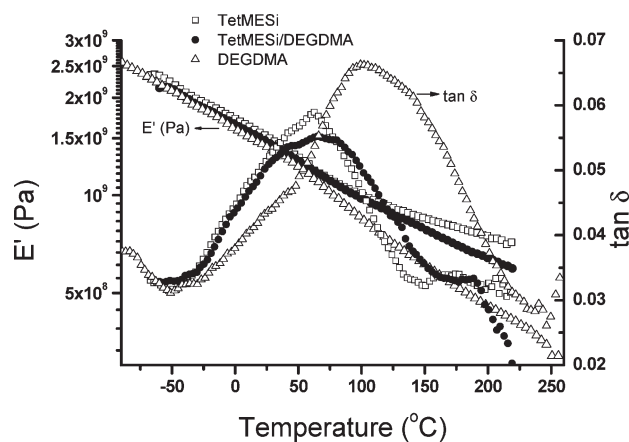


Figure 8. DMTA of the polymers from TetMESi, DEGDMa, and the 50/50 copolymer. Data points have been removed to improve the clarity of the figure.

0.055–0.07, which is approximately one-tenth of that normally observed with linear and lightly cross-linked polymers. This behavior is probably due to the small amount of molecular movement available in the network structure which reduces the intersegmental friction.^{48,49}

During water uptake, specimens containing TetMESi became soft as a result of the hydrolysis of the Si–O–C links, which reduced the cross-link density and also due to the hydroplasticization of the polymer. Figure 9 shows this behavior for the hydrolyzed and water-saturated material. The $\tan \delta$ curve shows a maximum corresponding to the inflection in the modulus curve at approximately 30 °C and a corresponding maximum in G'' at -10 °C, apparently due to the glass transition of the water vapor-saturated poly-HEMA polymer. This is in agreement with the data of Kolarik and Janacek⁴² who reported a maximum in G'' (1 Hz) near -10 °C in water-saturated (46% water uptake) due to the glass transition. However, the drop in the real modulus curve in Figure 9 is very broad and at approximately 105 °C another $\tan \delta$ maximum is observed. This is due to the effect of water evaporation from the wet poly-HEMA sample during the DMTA experiment, which causes the specimen

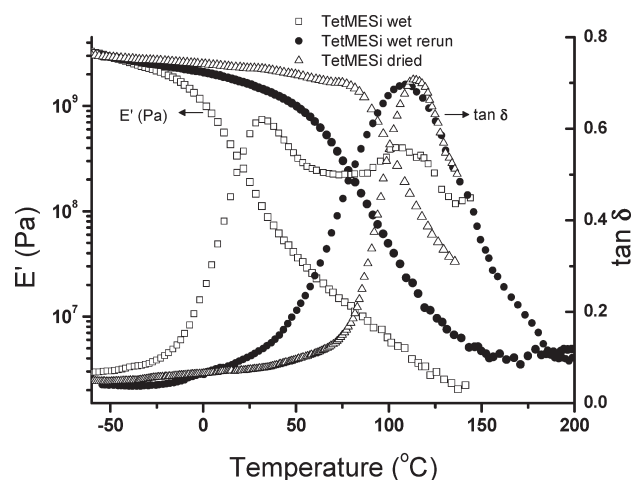


Figure 9. DMTA of polymerized TetMESi: (1) after equilibrium exposure to saturated water vapor, (2) after repeating the DMTA test on the same sample, and (3) after repeating the DMTA test on an identical sample after drying under vacuum at 60 °C for 24 h. Data points have been removed to improve the clarity of the figure.

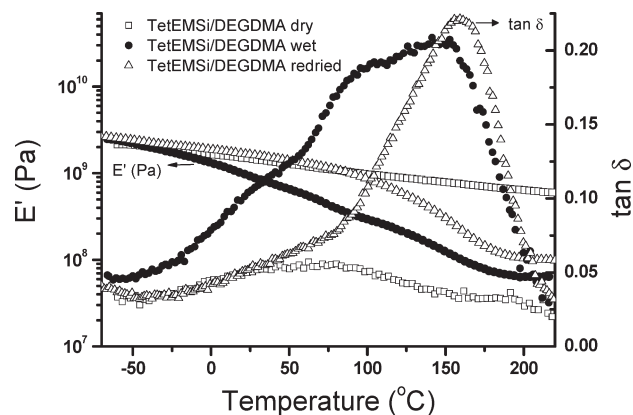


Figure 10. DMTA of copolymerized 50/50 TetMESi/DEGDMa: (1) as a dry sample, (2) after equilibrium exposure to saturated water vapor, and (3) after redrying under vacuum at 60 °C for 24 h. Data points have been removed to improve the clarity of the figure.

to vitrify (especially in the outer surfaces of the flexural specimen that contribute most to the overall DMTA behavior) and thus exhibit a second glass transition of the dry poly-HEMA; the modulus data do not show a corresponding change in slope, but this may be obscured by the apparent breadth of the overall transition. This explanation is confirmed by a subsequent rescan of the same specimen in the DMTA; in this second test the low temperature $\tan \delta$ peak is absent and only a broad curve with a peak near 105 °C is observed. When an identical specimen, which had been fully hydrolyzed and hydrated, was then dried under vacuum at 60 °C for 24 h, a much sharper $\tan \delta$ curve was observed with the $\tan \delta$ peak shifted to the higher temperature of 114 °C and a maximum in the loss modulus at 90 °C. These values are similar to that of 109 °C ($\tan \delta_{\max}$ 0.3 Hz) found by Dimarco et al.⁴¹ and that of 110 °C (G''_{\max} , 1 Hz) by Kolarik and Janacek⁴² for dry poly-HEMA.

Similar behavior was observed for the 50:50 wt % copolymer of TetMESi and DEGDMa (see Figure 10). Here, the highly cross-linked, unhydrolyzed copolymer had a broad transition

with little change in modulus and low $\tan \delta$. On hydrolysis the $\tan \delta$ increased significantly due to the greater amount of molecule movement available in the less highly cross-linked material, as discussed above, and three transitions appear to be present due to the effect of water loss changing the viscoelastic behavior of the polymer as the temperature increases. In addition, the storage modulus shows a larger decrease and the existence of a rubbery plateau due to the fewer cross-links in the copolymer. When this hydrolyzed polymer was redried, the damping behavior is dominated by one main glass transition at about 160 °C due to the dry copolymer of HEMA and DEGDMA. In contrast, the viscoelastic behavior of the water-saturated poly-DEGDMA specimen and of this specimen after drying was similar to that for the virgin material shown in Figure 8 because its structure is not significantly affected by water absorption.

CONCLUSIONS

The rate and final conversion of isothermal photopolymerization kinetics of a tetramethacrylate silane (TetMESi) monomer and its copolymerization with diethylene glycol dimethacrylate increase with raised curing temperature due to its effect on the propagation rate constant and the molecular mobility of the networks but full conversion is not attained due to topological restrictions on the methacrylate groups or chain radicals. The resulting materials have glass transition regions of low damping and with breadths of over 200 °C. In addition, the modulus of the materials does not show an abrupt drop in the glass transition and at 200 °C it is still above 0.5 GPa.

As confirmed by NMR studies of the monomer and FTIR studies of the polymer, exposure of poly-TetMESi to water vapor slowly causes hydrolysis of the Si–O–CH₂ bonds and water sorption studies show that poly-TetMESi absorbs ~30% water at equilibrium due partly to the consumption of water in the hydrolysis reaction but primarily due to swelling of the poly-HEMA. As a result of this, the dynamic mechanical properties of the hydrolyzed polymers were changed dramatically and the T_g reduced by water plasticization and loss of cross-links but drying of these polymers raised the T_g again.

Absorption of water by polymers containing TetMESi also caused the production of nanoscale particles or structures, as observed by the appearance of scattering in the UV–vis spectra.

From these results it may be concluded that these types of silicon-containing polymers may be useful for relatively transparent, low damping, high temperature, but anhydrous, applications or for cross-linked adhesives which require high modulus initially but which loose stiffness on exposure to water.

AUTHOR INFORMATION

Corresponding Author

*E-mail: wayne.cook@eng.monash.edu.au.

Notes

[†]Here the term “functional group” means the reactive group on the monomer molecule and “multifunctional” means a monomer with more than one functional group.

ACKNOWLEDGMENT

We acknowledge the financial support by the Australian Research Council Discovery Grant DP1093217 for research funding and for travel support for M.U. to Monash University,

and we also express appreciation for a Monash 2009 European Travel Grant which facilitated the visit of M.S. to Monash University.

REFERENCES

- (1) Sanchez, C.; Ribot, F. *New J. Chem.* **1994**, *18*, 1007–1047.
- (2) Tan, B.; Pan, H. M.; Irshad, H.; Chen, X. H. *J. Appl. Polym. Sci.* **2002**, *86*, 2135–2139.
- (3) Park, H. S.; Yang, I. M.; Wu, J. P.; Kim, M. S.; Hahn, H. S.; Kim, S. K.; Rhee, H. W. *J. Appl. Polym. Sci.* **2001**, *81*, 1614–1623.
- (4) Priola, A.; Gozzelino, G.; Ferrero, F. *Int. J. Adhes. Adhes.* **1990**, *10*, 77–80.
- (5) Pope, E. J. A.; Mackenzie, J. D. *J. Non-Cryst. Solids* **1986**, *87*, 185–198.
- (6) Buckley, A. M.; Greenblatt, M. *J. Chem. Educ.* **1994**, *71*, 599–602.
- (7) Brinker, C. J.; Scherer, G. W. *Sol-gel science: the physics and chemistry of sol-gel processing*; Academic Press: Boston, 1990; Part 1, p 112.
- (8) Schubert, U.; Hüsing, N. *Synthesis of inorganic materials*, 2nd ed.; Wiley-VCH: Weinheim; New York, 2004; Chapter 4.
- (9) McCormick, A. Recent progress in the study of the kinetics of sol-gel SiO₂ synthesis reactions. In *Sol-Gel Processing and Applications*; Attia, Y. A., Ed.; Plenum Press: New York, 1994.
- (10) Brinker, C. J.; Clark, D. E.; Ulrich, D. R. *Symposium on Better Ceramics Through Chemistry II Held in Palo Alto, California, on April 15–19, 1986*; Materials Research Society: Pittsburgh, PA, 1986; Vol. 73.
- (11) Novak, B. M.; Davies, C. *Macromolecules* **1991**, *24*, 5481–5483.
- (12) Ellsworth, M. W.; Novak, B. M. *J. Am. Chem. Soc.* **1991**, *113*, 2756–2758.
- (13) Novak, B. M. *Adv. Mater.* **1993**, *5*, 422–433.
- (14) Wei, Y.; Yang, D. C.; Bakthavatchalam, R. *Mater. Lett.* **1992**, *13*, 261–266.
- (15) Davidson, R. S.; Ellis, R.; Tudor, S.; Wilkinson, S. A. *Polymer* **1992**, *33*, 3031–3036.
- (16) Batten, R. J.; Davidson, R. S.; Ellis, R. J.; Wilkinson, S. A. *Polymer* **1992**, *33*, 3037–3043.
- (17) Novak, B. M.; Ellsworth, M. W. *Mater. Sci. Eng., A* **1993**, *162*, 257–264.
- (18) Wei, Y.; Wang, W.; Yang, D. H.; Tang, L. G. *Chem. Mater.* **1994**, *6*, 1737–1741.
- (19) Novak, B. M.; W., E. M.; Verrier, C., Nanostructured Organic Inorganic Hybrid Materials Synthesized Through Simultaneous Processes. In *Hybrid Organic-Inorganic Composites*; American Chemical Society: Washington, DC, 1995; Vol. 585, pp 86–96.
- (20) Kloosterboer, J. G.; Touwslager, F. J. Method of preparing a composite material of silica network and chains of a polyhydroxy compound and a liquid crystal display device incorporating such composite material. US Patent 5437896-A, 1995.
- (21) Wei, Y.; Jin, D. L.; Yang, C. C.; Wei, G. *J. Sol-Gel Sci. Technol.* **1996**, *7*, 191–201.
- (22) Yoshinaga, I.; Katayama, S. *J. Sol-Gel Sci. Technol.* **1996**, *6*, 151–154.
- (23) Spange, S.; Grund, S. *Adv. Mater.* **2009**, *21*, 2111–2116.
- (24) Innocenzi, P.; Brusatin, G.; Guglielmi, M.; Bertani, R. *Chem. Mater.* **1999**, *11*, 1672–1679.
- (25) Matejka, L.; Dusek, K.; Plestil, J.; Kriz, J.; Lednický, F. *Polymer* **1999**, *40*, 171–181.
- (26) Weast, R. C.; Chemical Rubber, C. *Handbook of chemistry and physics: a ready-reference book of chemical and physical data*; CRC Press: Cleveland, OH, 1973.
- (27) Cook, W. D. *Polymer* **1992**, *33*, 600–609.
- (28) Tong, L. K. J.; K., W. O. *J. Am. Chem. Soc.* **1945**, *67*, 1278–1281.
- (29) Horie, K.; Hiura, H.; Sawada, M.; Mita, I.; Kambe, H. *J. Polym. Sci., Part A: Polym. Chem.* **1970**, *8*, 1357–1372.
- (30) Cook, W. D. *Polymer* **1992**, *33*, 2152–2161.
- (31) Scott, T. F.; Cook, W. D.; Forsythe, J. S. *Polymer* **2002**, *43*, 5839–5845.

- 551 (32) Rozenberg, B. A. *Adv. Polym. Sci.* **1986**, 75, 113–165.
552 (33) Wisanrakkit, G.; Gillham, J. K. *J. Coat. Technol.* **1990**, 62, 35–50.
553 (34) Loshak, S.; Fox, T. G. *J. Am. Chem. Soc.* **1953**, 75, 3544–3550.
554 (35) Oleinik, E. F. *Adv. Polym. Sci.* **1986**, 80, 49–99.
555 (36) Cook, W. D. *J. Polym. Sci., Part A: Polym. Chem.* **1993**,
556 31, 1053–1067.
557 (37) Soh, S. K.; Sundberg, D. C. *J. Polym. Sci., Part A: Polym. Chem.*
558 **1982**, 20, 1299–1313.
559 (38) Stickler, M. *Macromol. Chem. Phys.* **1983**, 184, 2563–2579.
560 (39) Socrates, G. *Infrared and Raman Characteristic Group Frequen-*
561 *cies - Tables and Charts*, 3rd ed.; John Wiley and Sons Ltd.: New York,
562 2001.
563 (40) Hodge, R. M.; Simon, G. P.; Whittaker, M. R.; Hill, D. J. T.;
564 Whittaker, A. K. *J. Polym. Sci., Part B: Polym. Phys.* **1998**, 36, 463–471.
565 (41) Dimarco, G.; Lanza, M.; Pieruccini, M. *Nuovo Cimento Soc. Ital.*
566 *Fis., D* **1994**, 16, 849–854.
567 (42) Kolarik, J.; Janacek, J. *J. Polym. Sci., Part B: Polym. Phys.* **1972**,
568 10, 11–22.
569 (43) Sideridou, I. D.; Karabela, M. M. *J. Appl. Polym. Sci.* **2008**,
570 109, 2503–2512.
571 (44) D'Agostino, A.; Colella, M.; De Rosa, M.; De Rosa, A.; Lanza,
572 A.; Schiraldi, C. *J. Polym. Res.* **2009**, 16, 561–567.
573 (45) Bohren, C. F.; Huffman, D. R. *Absorption and scattering of light*
574 *by small particles*; John Wiley and Sons: New York, 1983.
575 (46) Zhou, S. X.; Wu, L. M.; Sun, J.; Shen, W. D. *Prog. Org. Coat.*
576 **2002**, 45, 33–42.
577 (47) Alfrey, T. G., E.F.; Lloyd, W. G. *J. Polym. Sci., Part C: Polym. Lett.*
578 **1966**, 12, 249–261.
579 (48) Andrady, A. L.; Sefcik, M. D. *J. Polym. Sci., Part B: Polym. Phys.*
580 **1983**, 21, 2453–2463.
581 (49) Sauer, J. A. *J. Polym. Sci., Part C: Polym. Lett.* **1971**, 32, 69–122.